Available online at www.sciencedirect.com
SCIENCE DIRECT®
Dyes and Pigments 63 (2004) 101–113
DYES and PIGMENTS
www.elsevier.com/locate/dyepig

Acid alizarin violet interactions with surfactants: ionization and thermodynamic parameters in buffered cationic, anionic and nonionic surfactant solutions

M. Dakiky[a], A. Manassra[a], M. Abdul Kareem[a], F. Jumean[b], M. Khamis[a,1,*]

[a]*Faculty of Science & Technology, Al-Quds University, P.O.B. 20002, East Jerusalem*
[b]*Department of Biology and Chemistry, American University of Sharjah (AUS), P.O.B. 26666, Sharjah, United Arab Emirates*

Received 1 September 2003; received in revised form 30 November 2003; accepted 2 December 2003

Abstract

Proton ionization constants for Acid alizarin violet N (AVN) were obtained in micellar solutions by spectrophotometry. The effect of addition of three surfactants, CTAB, TX-100 and SDS, was investigated in buffered solutions in the pH range 2.0–13.0. Enthalpies and entropies for the second proton ionization were evaluated by the thermochromic method. At 25 °C, in the absence of surfactant, pK_2' and pK_3' for AVN were 7.00 and 12.80, respectively. At concentrations above CMC, CTAB caused a decrease in these values to 6.35 and 12.56, whereas TX-100 led to an increase to 8.09 and 13.04. With SDS, changes were not pronounced. Results were explained on the basis of hydrophobic and electrostatic interactions between AVN and the micelle, taking into account possibilities of short or deep penetration mechanisms of AVN into micelle. In addition to their effect on pK, these micelles significantly altered enthalpy and entropy of ionization values. Finally, association constants for the acidic and basic forms of AVN with each surfactant were obtained and the results interpreted in terms of dye–micelle interactions.

Keywords: Alizarin; Ionization; Surfactants; Thermodynamics; Azo dyes

1. Introduction

Azo dyes are an interesting class of compounds that are widely used in chemistry and technology [1–4]. They exhibit a range of colours, good fastness properties and tinctorial strength [5] and undergo tautomerization, giving several tautomers with different spectroscopic properties [3]. Hydroxy azo-dyes capable of undergoing azo–hydrazo tautomerization are those in which the hydroxyl group is conjugated to the azo group, i.e. in the *ortho* and *para* positions. Most azo phenol

* Corresponding author. Fax: +972-2-796960.
E-mail address: khamis@planet.edu (M. Khamis).
[1] On a sabbatical leave at the AUS.

0143-7208/$ - see front matter © 2004 Elsevier Ltd. All rights reserved.
doi:10.1016/j.dyepig.2003.12.014

dyes exist in the azo form because of the resonance stabilization energy of the aromatic ring system. The loss in energy in going from hydroxyl naphthalene to a naphtho quinone is less than in going from hydroxyl benzene to benzo quinone. Thus in azo-naphthol-dyes, the hydrazo form prevails [6,7]. This class is used in analytical chemistry as acid–base indicators [4] and as metal complexing agents for detecting low concentrations of metal ions. Hydrogen bonding, electrostatic interactions, van der Waal's forces and hydrophobic interactions, are all responsible for dye–dye self association [2]. Several methods have been used to study dye aggregation, but the spectrophotometric method is the most common [8–13]. Several species exist in equilibrium (azo-enol ↔ hydrazoketone) and (monomer ↔ dimer). These equilibria are sensitive to dye concentration, temperature and solvent [14].

Special attention was given to the study of changes in both the acid–base and optical properties of a dye in aqueous and micellar solutions [15–18]. The effect of surfactant addition can be studied below, at, and above the critical micellar concentration (CMC). The effect of cationic, anionic and nonionic surfactants on some *O*,*O*′dihydroxy-azo-dyes was investigated [19]. In the case of *O*,*O*′dihydroxy-azo-dyes, spectral changes were explained on the basis of selective solubilization, hydrophobic interactions and concentration effect in the micellar pseudophase. Several mechanisms have been proposed to explain the enhancement of solubility of the organic compounds in general, and azo dyes in particular, in surfactants [19–22]. Models of interactions have been proposed in which the observed changes were attributed to the change in the microenvironment of the dye resulting from its incorporation inside the micelle [14,19].

Previous studies by Dakiky et al. on methyl orange, the parent azo dye, found that solubilization of the dye inside various types of micelles resulted in drastic changes in the thermodynamic parameters for the ionization of the azo bound proton [21,22]. For dyes that contain additional ionizable protons, the presence of a surfactant was sometimes found to exert an opposite effect on p*K*s [23]. Interactions between cationic surfactants and cationic dyes are predominantly hydrophobic [24]. Non-coulombic interactions also play a role in the complex formation between oppositely charged dyes and surfactants [25].

The effect of the length of the alkyl chain of a surfactant on the complex formation between cationic surfactants and acid dyes has been studied [25]. The results indicate that hydrophobicity of alkyl chains plays an important role in complex formation. In addition, high hydrophobicity of aromatic acid dyes was found to enhance their ability to form a complex with cationic surfactants. The large affinity of the dye for cationic polar heads is attributed to the interaction between π-electrons and the positive charge [26]. Molar absorbtivity of micellar–dye solutions was studied and used in improving the sensitivity of calorimetric determination of aryl amines via diazotization and coupling [27]. Finally, it may be stated that formation of dye–surfactant ion pairs is the consequence of mutual influences of electrostatic forces and hydrophobic interactions, with some other short-range attractive forces [28].

In an attempt to better understand the dye–surfactants interaction, this work studies the spectroscopic properties, thermodynamic ionization parameters, and association constants of AVN with micelles of CTAB, TX-100 and SDS. The values are then compared to those for methyl orange [22] and other dyes [23,24].

2. Experimental

2.1. Materials

Acid alizarin violet N (4-hydroxy-3-(2-hydroxy-1-naphthyl azo) benzene sulphonic acid) is also known as Acid Chrome Violet K, C.I 15670. It was obtained from Aldrich as sodium salt ($C_{16}H_{11}O_2N_2SO_3Na$) and purified by recrystallization from ethanol. TX-100 (*p*-octyl-phenol (oxyethene)$_n$, $n = 9.5$), SDS (sodium dodecyl sulphate), and CTAB (cetyl-trimethyl-ammonium bromide) were Sigma chemicals and were used without further purification. CMC for CTAB [29], SDS [29] and TX-100 [20] are 1×10^{-3}, 8×10^{3} and

2×10^{-3} M, respectively. Phosphoric acid, acetic acid and boric acid, were all of analytical grade.

2.2. Methods

Thermochromic measurements were performed on a Helios α-Unicam spectrophotometer equipped with a thermostated cell compartment. The instrument was controlled by Vision software via an RS-232 real time interface. The temperature inside the cell was controlled by DBS (PCB 150) Peltier and measured to within ±0.1 °C by a thermocouple immersed in the cell. Other absorption measurements were carried out using a λ-5 Perkin–Elmer spectrophotometer equipped with a thermostated cell compartment. pH measurements were recorded on a Jenway 3310 pH meter. Measurements were carried out on 6.80×10^{-5} M dye solutions in the pH range 2–13. The ionic strength was maintained at 0.100 M. For pK measurements, spectra were recorded at 25 °C in the range 300–750 nm. The thermochromic method [22,30,31] was employed to obtain the ionization parameters for the second proton of AVN, before and after surfactant addition. Measurements were made at, or slightly above, the CMC in the presence of 0.033 M phosphate buffer. The pH of each solution was adjusted to a value close to the pK_2 of AVN. Repetitive scans were recorded in the wavelength range of 350–700 nm and in the interval 10–55 °C. Spectra of most acidic (pH = 3) and most basic (pH = 10) solutions were also recorded within this range. Association constants were determined at 25 °C by analysis of the spectra of AVN solutions at several micelle concentrations, using established procedures [22,32].

3. Results and discussion

3.1. Proton ionization constants

AVN has two bulk moieties, the phenyl group and the naphthyl group. Two hydroxyl groups are located in *ortho* positions to the azo group. The one attached to the phenyl moiety is the more acidic. In aqueous solution AVN can exist either in the azo- or hydrazo-forms, each capable of forming three distinct species through stepwise proton ionizations (Fig. 1). Additionally, monomer–dimer equilibrium exists at low pH. The third proton ionization, due to the naphthol proton, occurs only in very basic media, in which AVN is present mostly in the hydrazo form. In this form, the naphthol proton is located at the nitrogen atom of the azo group. Hydrazo protons are known to be very weakly acidic, i.e. pK_3 is very high [2,3,14,33].

Fig. 2 shows visible spectra of AVN as a function of pH in aqueous buffer and in buffered solutions containing micellar concentrations of CTAB, TX-100 and SDS. At pH < 10 and in the absence of surfactant, absorbance maxima are observed at 500 and 560 nm (Fig. 2a). These can be assigned to H_2In^- and HIn^{2-}, respectively. A slightly distorted isobestic point is located at 525 nm. H-NMR and spectrophotometric studies on similar polyprotic azo dyes [14] have led to the conclusion that they exist predominantly as dimers at pH < 4. Moreover, dissociation to monomers is typically accompanied by the appearance of a shoulder at a higher wavelength. Fig. 2a shows that, in addition to favoring the basic form, a rise in pH promotes dissociation to monomers as evidenced by a bathochromic acid band broadening. Addition of CTAB causes profound spectral changes (Fig. 2b) with the basic band shifted to 600 nm and a shoulder appearing at 530 nm. TX-100 had similar, but less pronounced effects with a basic band maximum at 589 nm and a shoulder at 530 nm (Fig. 2c). By contrast, SDS addition was not accompanied by significant changes (Fig. 2d).

AVN can be represented as H_2In^-, in which the negative sign arises from the dissociation of the highly acidic sulphonate proton. Thus pK_2' and pK_3' refer to the following dissociation steps (Fig. 1):

$$H_2In^- \leftrightarrow H^+ + HIn^{2-} \quad (1)$$

$$HIn^{2-} \leftrightarrow H^+ + In^{3-} \quad (2)$$

For the ionization of the second proton (Eq. (1)), it can be readily shown that absorbance, A, depends on pH according to

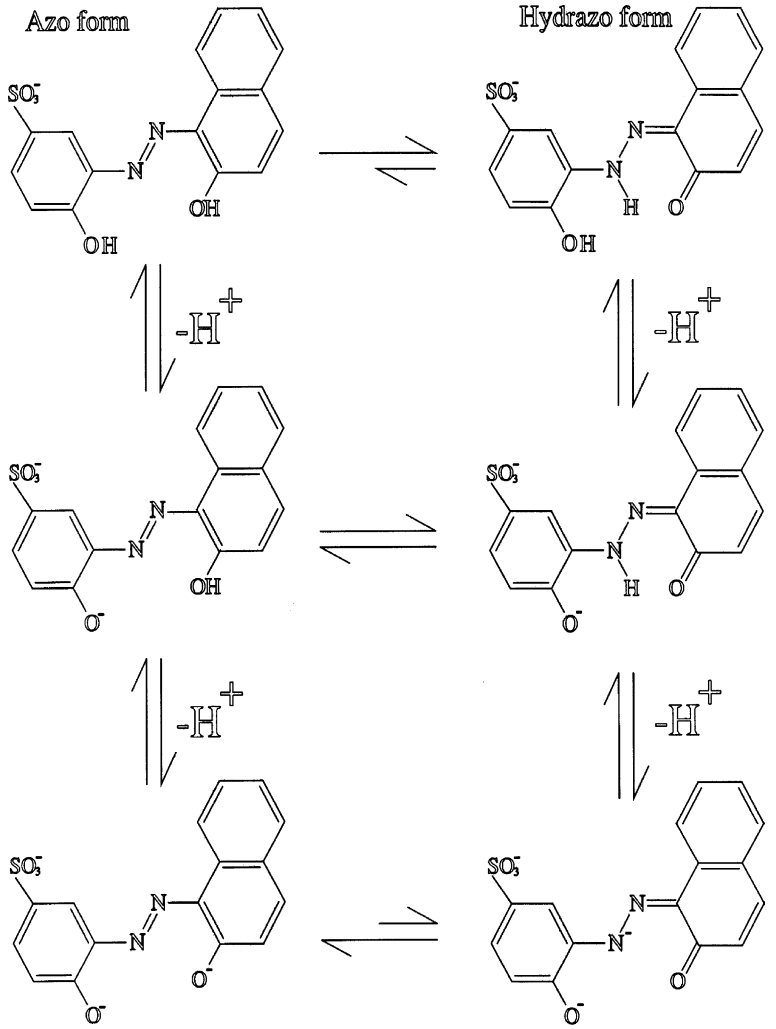

Fig. 1. Ionization steps of azo- and hydrazo-forms of AVN.

$$\mathrm{pH} = \mathrm{p}K_2' + \log R \tag{3}$$

where $R = (A - A_a)/(A_b - A)$, A_a and A_b are absorbances of most acidic and basic solutions, both of which are obtained from a plot of A vs. pH. A typical example is shown in Fig. 3. From Eq. (3), a plot of pH vs. log R at wavelengths where A is sensitive to pH yields $\mathrm{p}K_2'$. Fig. 4 gives plots for the four environments investigated and their $\mathrm{p}K_2'$ values are listed in Table 1.

For the calculation of $\mathrm{p}K_3'$, Fig. 3 shows that it is not possible to assign directly a value to A_b (the absorbance of In^{3-}). Thus an equation for $\mathrm{p}K_3'$, similar to Eq. (3), could not be used in this case. K_3' was accordingly obtained by a linearization procedure [22] of Eq.(3). This procedure yields the equation:

$$[H^+](A_a - A) = K_3'A - A_bK_3' \tag{4}$$

A plot of $[H^+](A_a - A)$ vs. absorbance, A, results in a straight line with the slope equal to K_3'. A typical plot is presented in Fig. 5 and $\mathrm{p}K_3'$ values are listed in Table 1.

The $\mathrm{p}K_2'$ values listed in Table 1 are averages of those obtained at four analytical wavelengths in the range 470–600 nm. The standard deviation (σ)

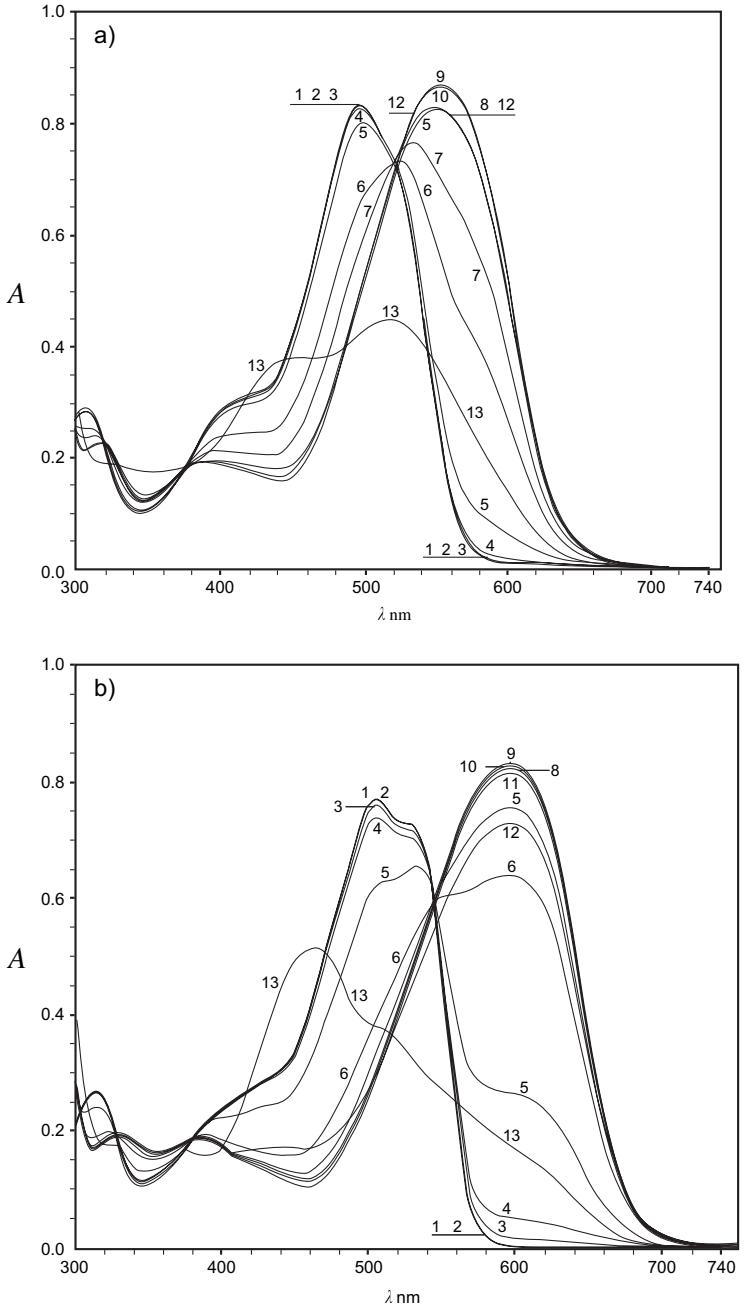

Fig. 2. (a–d) Absorption spectra of 6.8×10^{-5} M AVN in (a) buffer, and buffered solutions containing (b) CTAB, (c) TX-100 and (d) SDS. $T = 25.0\,^{\circ}C$, $\mu = 0.100$ M. Numbers from 1 to 13 refer to pH values 2.20, 3.20, 4.10, 5.02, 6.05, 7.00, 7.45, 8.25, 9.10, 10.25, 11.15, 12.10 and 13.10, respectively.

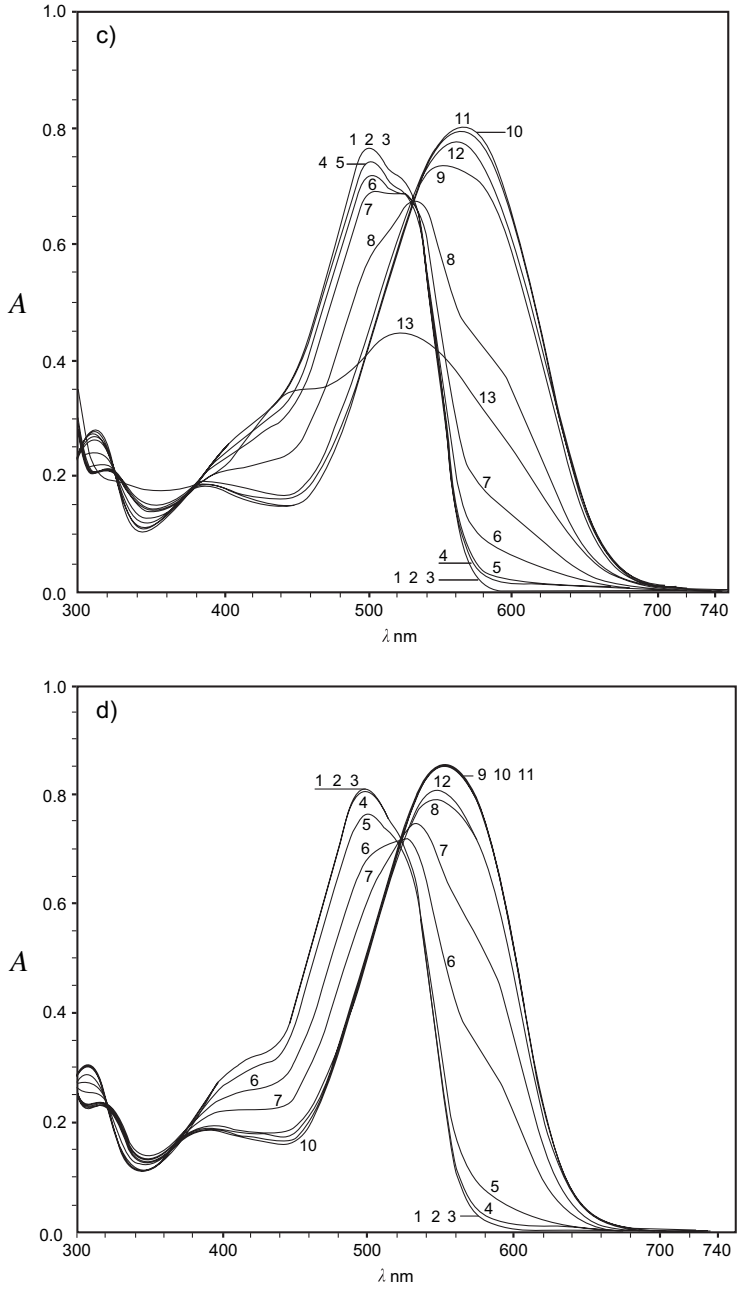

Fig. 2 (*continued*).

varied between 0.01 and 0.05 units. Above CMC, the change in pK_2' due to the addition of surfactant, ($\Delta pK_2'$), is −0.6, +1 and 0.1 for CTAB, TX-100 and SDS, respectively. The lowering of pK_2' by CTAB micellar solution can be explained on the basis of electrostatic attraction between AVN species of the HIn^{2-} type and the positive cationic heads of CTAB. Here, the organic part of AVN is solubilized into the micellar core of CTAB, whereas the $-SO_3^-$

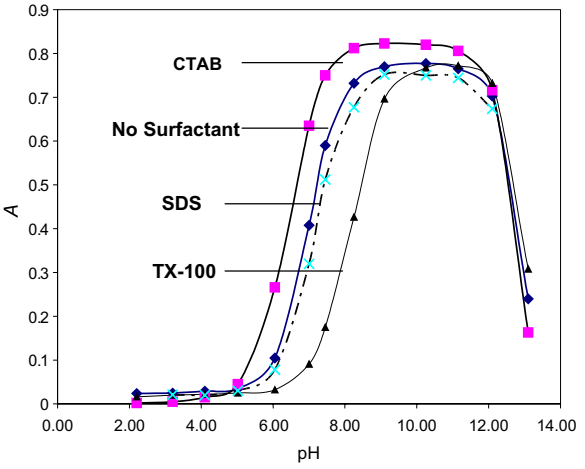

Fig. 3. Plot of absorbance vs. pH for 6.8×10^{-5} M AVN, $\mu = 0.100$, $T = 25$ °C, $\lambda = 580$ nm.

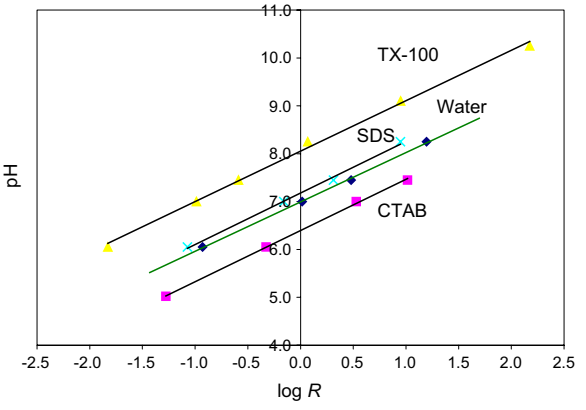

Fig. 4. Plot of pH vs. log R for 6.8×10^{-5} M AVN in the four media. $\mu = 0.100$ M, $T = 25.0$ °C. For CTAB, $\lambda = 580$ nm; for all others $\lambda = 560$ nm.

and −OH groups lie within the Štern layer oriented near the micelle surface. This is consistent with a short penetration mechanism that leads to sharp and selective deprotonation [19]. However, the decrease in pK_2' at concentrations below the CMC (1×10^{-3} M), can be attributed to the formation of the ion pair HIn^{-2}–CTAB. With TX-100, the rise in pK_2' is probably due to the arrangement of dye molecules within the micelles. Here, hydrogen bonding between the phenoxy proton of AVN and the ether moieties of TX-100 stabilizes the acidic form (H_2In^-) relative to the basic (HIn^{2-}) form, thus leading to the observed rise in pK_2'. Finally, the relatively small increase of pK' values observed with SDS can be attributed to the existence of the repulsive electrostatic interactions, between the negatively charged species of SDS and AVN, and the opposing stabilizing effect of hydrophobic interactions between the organic portions of these species. The negatively charged head groups of SDS are expected to destabilize the ionized form (HIn^{2-}), thereby leading to an increase in pK_2'. Hydrophobic interactions, on the other hand, can promote the accommodation of AVN inside SDS. However, the observed change of only +0.1 units is significantly lower than increments observed with other azo dyes [19,22].

The pK_3' values obtained are averages from data obtained at two different analytical wavelengths between 480 and 600 nm with standard deviation estimated to be 0.04 units. The pK_3' value for AVN in the presence of SDS could not be estimated due to the precipitation of SDS at the pH range in vicinity of ionization. For both CTAB and TX-100, $\Delta pK_3'$ follows a similar trend to that observed for pK_2'. $\Delta pK_3'$ values are −0.2 for CTAB and 0.2 for TX-100 above CMC. These changes are in line with the explanations offered earlier for changes in pK_2'.

3.2. Enthalpies and entropies of ionization

In applying the thermochromic method [22,30,31], visible spectra of AVN in phosphate buffer were recorded over the temperature range 10–55 °C. An analytical wavelength is then selected for calculation of thermodynamic values. The criteria for selection are sensitivity to temperature changes and that the band be ascribed to well-defined species. For each temperature, the term R (Eq. (3)) is evaluated. Log R values are then fitted to an expression of the form:

$$\text{Log } R = a/T - b + cT \tag{5}$$

The constants a, b and c are obtained from regression analysis. The above equation was derived with the assumption that the pKs of both buffer and dye vary according to $pK = a/T - b + cT$,

Table 1
Effect of surfactants on pK_2' and pK_3' of AVN at 25.0 °C, $\mu = 0.100$ M

Surfactant	[Surfactant], M	pK_2'	pK_3'
None		7.00	12.80
CTAB	5.00×10^{-4}	6.45	12.61
CTAB	9.00×10^{-4}	6.35	12.60
CTAB	5.00×10^{-3}	6.40	12.62
CTAB	1.00×10^{-2}	6.40	12.56
TX-100	1.90×10^{-5}	6.99	12.76
TX-100	6.00×10^{-5}	7.03	12.76
TX-100	1.90×10^{-4}	7.05	12.81
TX-100	3.50×10^{-4}	7.21	13.00
TX-100	2.00×10^{-3}	7.93	13.00
TX-100	4.00×10^{-3}	8.09	13.04
SDS	7.80×10^{-5}	7.01	–
SDS	1.00×10^{-4}	7.02	–
SDS	1.40×10^{-3}	7.04	–
SDS	3.00×10^{-3}	7.03	–
SDS	7.80×10^{-3}	7.09	–
SDS	1.50×10^{-2}	7.14	–

differing only in the value of the constants. It was further assumed that the activity ratio of buffer species (a_B^-/a_{HB}) and the activity coefficient ratio of indicator species (γ_D^-/γ_{HD}) are independent of temperature. Eqs. (6) and (7) follow from Eq. (5) by direct differentiation and substitution into the van't Hoff relation [34], leading to change of enthalpy (ΔH) and entropy (ΔS) of ionization

$$\delta\Delta H = \Delta H_B - \Delta H_D = 2.303R(a - cT^2) \quad (6)$$

$$\delta\Delta S = \Delta S_B - \Delta S_D = 2.303R(b - 2cT) \quad (7)$$

The subscripts B and D refer to buffer and dye, respectively. Values of the constants a, b and c can be obtained from a regression fit of a plot of T log R vs. T. The values of $\delta\Delta H$ and $\delta\Delta S$ obtained in this work are apparent values, primed, since they pertain the solution at a finite ionic strength.

Thermochromic spectra for AVN in the four media contain contributions from the species involved in equilibria related to the second ionization step of AVN (Fig. 1). In order to selectively identify those spectral changes that are mainly due to the effect of temperature on proton ionization, the temperature dependence of the acidic form (pH = 3) and the basic form (pH = 10) was separately studied. The results indicated that only minor changes occur in the temperature range investigated. In particular, at $\lambda = 564$ nm for AVN in TX-100 and at $\lambda = 580$ nm for AVN in the remaining three media, no measurable changes

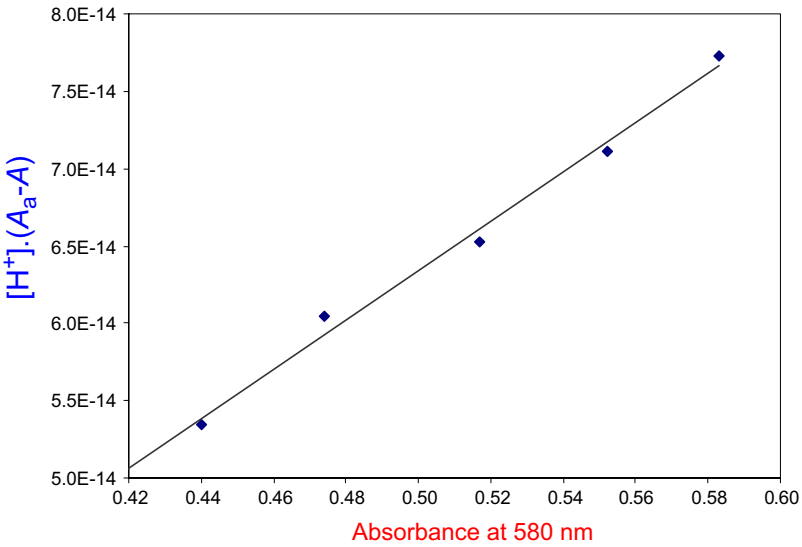

Fig. 5. Plot of $[H^+](A_a - A)$ vs. A for 6.8×10^{-5} M AVN. $T = 25.0$ °C, $\mu = 0.100$ M, $\lambda = 580$ nm.

were observed. Accordingly these wavelengths were selected for analysis of the thermochromic data.

Fig. 6 shows the effect of temperature on AVN solutions whose pH values are in the vicinity of the pK_2 of the dye. It is evident that a rise in temperature results in an absorbance increase for the basic form. However, there is a stark difference in the magnitude of the observed changes. For example, on going from 13 to 56 °C, the absorbance at λ_{max} (basic form) of a solution without surfactant added rose by 40%. However, that for solutions containing TX-100 and CTAB rose steeply, by 83% and 90%, respectively. By contrast, the rise with SDS was only 16% under the same conditions. The magnitude of thermochromic changes is relevant to the calculation of R and hence to the determination of $\delta\Delta H$ and $\delta\Delta S$ (Eqs. (6) and (7)). Specifically, a small thermochromic influence indicates that ΔH of ionization of AVN and phosphate buffer (as related to their pK_2's) are close in value, in the particular medium and at the same temperature conditions. In order to separate the temperature influence on phosphate from that on solutions containing phosphate and AVN, pK_2' measurements were made on

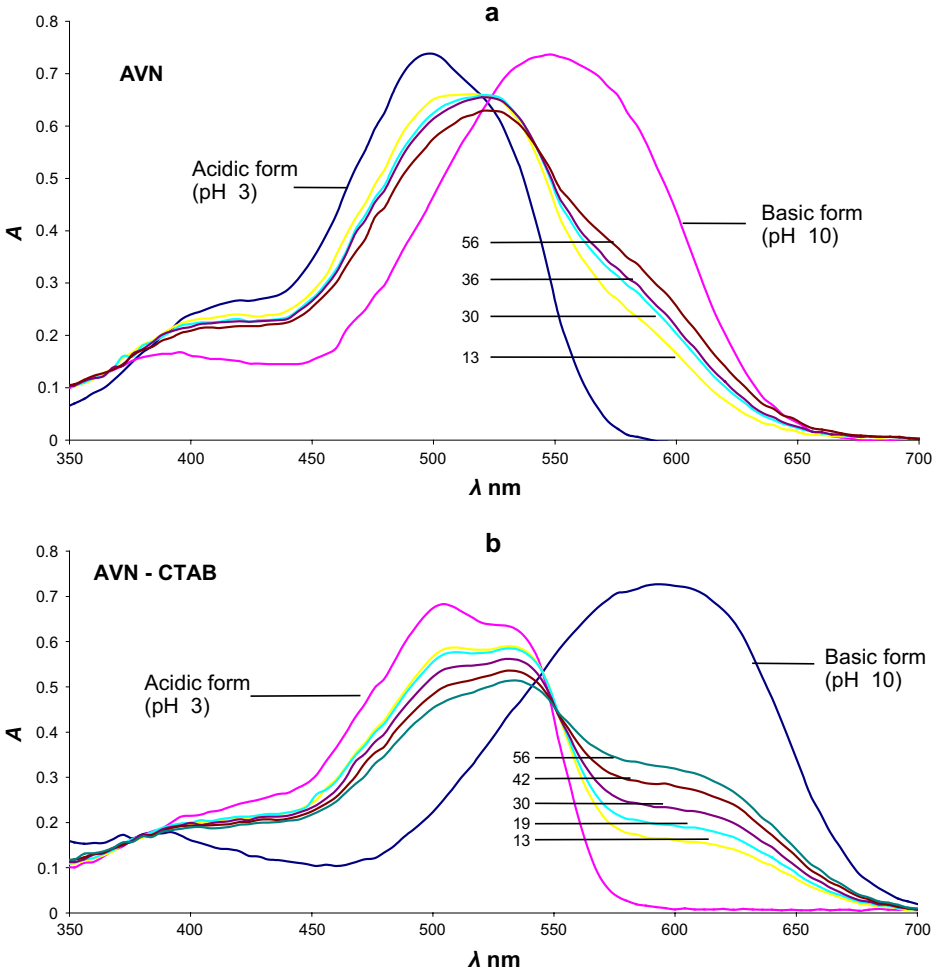

Fig. 6. Thermochromic spectra for buffered 6.8×10^{-5} M AVN in the four media (a) no surfactant, (b) CTAB, (c) TX-100 and (d) SDS. Temperatures are indicated. [CTAB] = 1.0×10^{-3} M, [TX-100] = 4.0×10^{-3} M and [SDS] = 8.0×10^{-3} M.

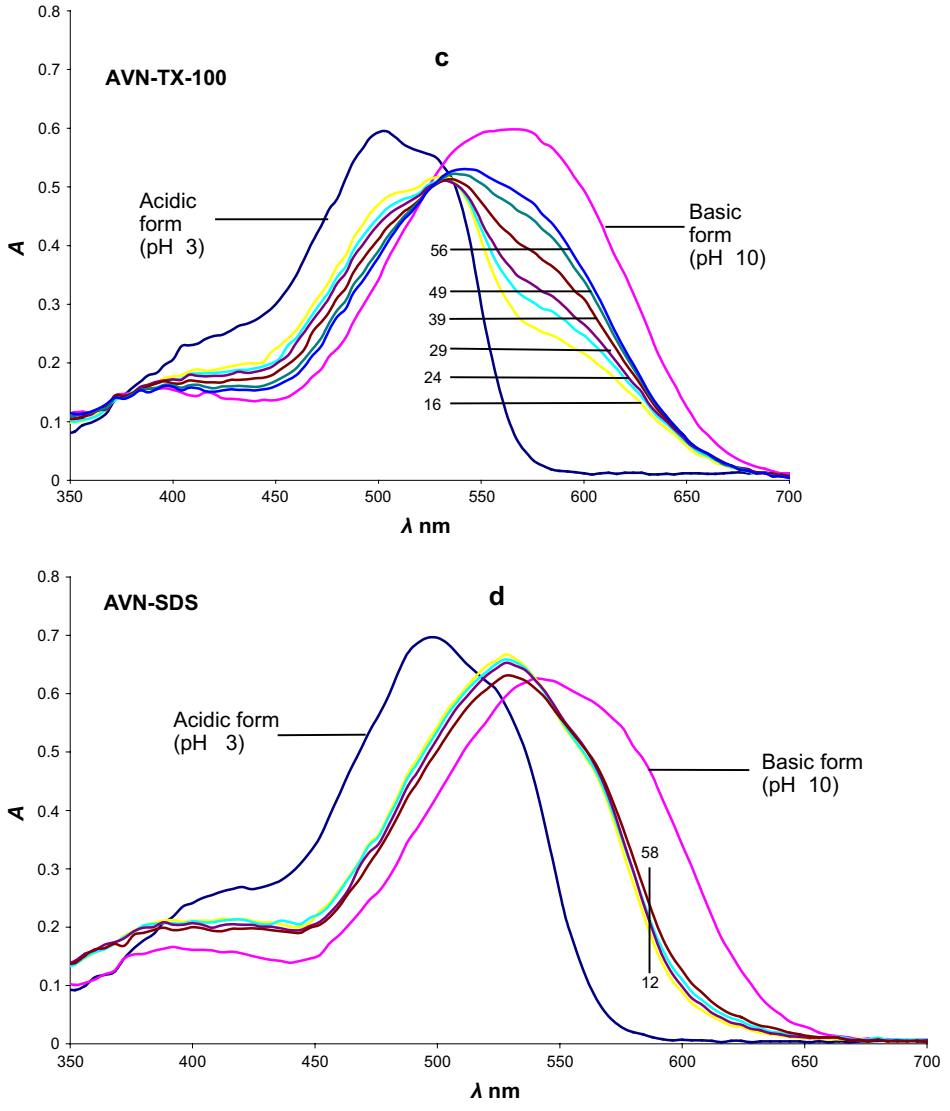

Fig. 6 (*continued*).

phosphate in all the four media, with $I = 0.100$ M, and in the temperature range 10–45 °C. The results indicate that, in the presence of the three surfactants above CMC, pK_2' changes for phosphate were within the standard deviation of 0.02 units. In addition, the temperature study revealed that, at all temperatures within the range investigated, no significant change in pK_2' of phosphate could be ascribed to the addition of any of the three surfactants.

Plots of $T \log R$ vs. T in each of the four media are shown in Fig. 7. The regression results are summarized in Table 2. As may be seen from the correlation coefficients (r^2) in this table, the data are well described by Eq. (5).

Since $\Delta H_B'$ and $\Delta S_B'$ for the second proton ionization of the phosphate buffer are known [35,36], the corresponding values for AVN in each the four environments can be obtained from the experimental $\delta\Delta H'$ and $\delta\Delta S'$ values by direct

substitution in Eqs. (6) and (7). These values are listed in Table 3. The tabulated standard $\Delta G'$ values have been obtained from those for the CMC values of pK'.

From Table 3, it is apparent that $\Delta G'$ is insensitive to SDS addition, whereas it is significantly raised by TX-100 and lowered by CTAB. Thus AVN ionization is enhanced by CTAB, retarded by TX-100 and almost unaffected by SDS. $\Delta G'$ is made of enthalpic ($\Delta H'$) and entropic ($\Delta S'$) contributions. Addition of CTAB and TX-100 causes an increase in $\Delta H'$ from 17.1 to 25.5 and 32.3 kJ mol^{-1}, and an increase in $\Delta S'$ from -76.7 to -29.9 and -45.0 J K^{-1} mol^{-1}, respectively. However, in the case of CTAB the increase in entropy more than offsets the enthalpic effect, with the result that $\Delta G'$ experiences a net large drop. With TX-100 the entropy change was not sufficient to counterbalance the large unfavorable increase in $\Delta H'$, with the result that $\Delta G'$ experienced an appreciable increase. By contrast, SDS addition drastically lowers $\Delta H'$, thereby making the enthalpic contribution to ionization more favorable. However, this effect is almost equally counterbalanced by the unfavorable entropy change, giving an essentially unchanged $\Delta G'$.

The above mentioned findings are in marked contrast to those obtained with methyl orange (MO), the parent azo dye [22]. In that case both $\Delta H'$ and $\Delta S'$ experienced large drops in the presence of micellar CTAB and TX-100, these being much more pronounced for the first surfactant. Both of these parameters, however, increased in the presence of SDS. The explanation of the MO findings was based on the ionization type $HIn^{\pm} = In^{-} + H^{+}$. Here, In^{-} experiences additional stabilization by electrostatic attraction to the positively charged groups on CTAB, whereas both $HIn^{\pm}$ and In^{-} are well solubilized in CTAB and TX-100 due to hydrophobic interactions. AVN differs from MO in two major respects: the first is electrostatic as can be seen from the AVN ionization type $H_2In^{-} = In^{2-} + H^{+}$; the second is structural. The net charge creation accompanying ionization of AVN renders this process less favorable than the MO case. Hence, the observed increase in both the enthalpy and entropy of ionization with the addition of CTAB and TX-100 (Table 3) suggests that the ionized AVN species interact more favorably, probably through H-bonding, in water than inside the micelle. The findings with SDS appear

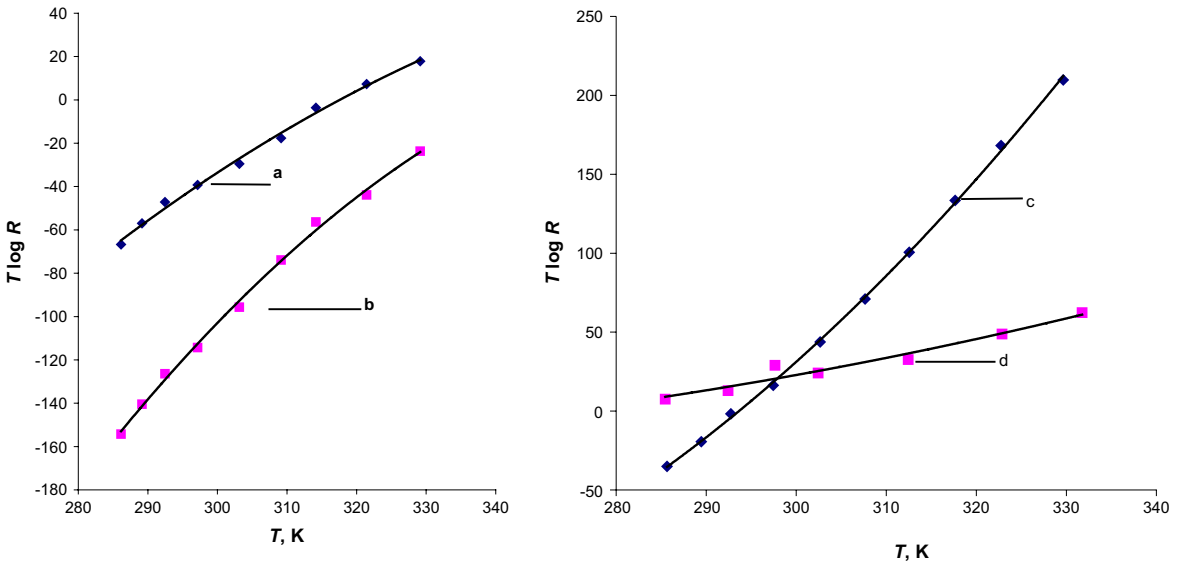

Fig. 7. Dependence of $T \log R$ on T for 6.8×10^{-5} M buffered AVN solutions in the four media (a) no surfactant, (b) CTAB, (c) TX-100 and (d) SDS. [CTAB] = 1.0×10^{-3} M, [TX-100] = 4.0×10^{-3} M and [SDS] = 8.0×10^{-3} M.

Table 2
Constants of Eq. (5) and correlation coefficients in the four media

System	a	b	c	(r^2)
AVN–no surfactant	−1648	−8.66	−0.0109	0.995
AVN–CTAB	−2994	−15.96	−0.0211	0.991
AVN–TX-100	1498	14.90	0.0334	0.956
AVN–SDS	216	2.31	0.0056	0.998

anomalous as they are contrary to what one would expect from electrostatic considerations alone. Here, it would appear that the electrostatic repulsion between In^{2-} and the negatively charged end groups of SDS is more than offset by stabilization due to hydrophobic interactions. The highly negative $\Delta S'$ value obtained in this case ($-100\,J\,K^{-1}\,mol^{-1}$), indicates the presence of highly ordered ionized species within the SDS micelles.

3.3. Association constants

The method for obtaining the association constant of the dye with micelles has been described [22,32]. Spectra were recorded for 6.8×10^{-5} M AVN in the presence of several surfactant concentrations of CTAB, TX-100 and SDS, at and above CMC. For all solutions, the ionic strength was adjusted to 0.100 M. Runs were made at pH 3 and pH 10. At these pHs AVN exists predominantly in the acidic form (H_2In^-) and the basic form (HIn^{2-}), respectively. The micelle concentration [M] for each solution was calculated by dividing the surfactant concentration by the aggregation number of the micelles close to the CMC. This number is 50 for TX-100 [20] and 80 for both SDS [37] and CTAB [38]. Absorbance values at high surfactant concentration ($A_m{}^\infty$), the lowest (CMC) surfactant concentration (A_a), and at intermediate surfactant concentrations (A) were substituted in Eq. (8). K_C' is obtained from the best linear fit of η versus 1/M

$$\eta = \frac{A_m^\infty - A_a}{A - A_a} = 1 + (K_C'[M])^{-1} \quad (8)$$

The association constants for both the acidic and basic forms of AVN with each of the three surfactants investigated are given in Table 4. All association constants lie within the same order of magnitude. However, values with CTAB are significantly higher. This can be explained on the basis of additional stabilization, which could arise from electrostatic attraction between negative AVN species and positive head groups in CTAB micelles. In this case, the association constant for the acid form of AVN is significantly higher than that of the base. This finding is contrary to what would be expected from electrostatic considerations alone, since the acid form has one less negative charge than the base. A plausible explanation for this apparent anomaly is that at pH 3 AVN dimerizes to a large extent, in line with the reported aggregation of azo dyes in acidic media [19]. The change in bulk properties accompanying dimerization may account for the observed behavior. Finally, the association constants with SDS are lower than those with TX-100. This is as expected from electrostatic repulsions between AVN and the negatively charged SDS head groups.

4. Conclusion

The solubilization of AVN in micellar CTAB, TX-100 and SDS was accompanied by profound changes in spectroscopic and thermodynamic

Table 3
Thermodynamic values for the second proton ionization of AVN in the four media, at 25 °C

System	$\Delta G' \pm 0.2$ (kJ mol^{-1})	$\Delta H' \pm 0.2$ (kJ mol^{-1})	$\Delta S' \pm 5$ (J K^{-1} mol^{-1})
AVN–no surfactant	40.0	17.1	−77
AVN–CTAB	34.2	25.5	−29
AVN–TX-100	45.6	32.3	−45
AVN–SDS	40.1	9.53	−100

Table 4
Apparent association constants (K_C'), at 25 °C, for the acidic and basic forms of AVN with the three micellar systems

System	$K_C' \times 10^{-3}$ acid form	$K_C' \times 10^{-3}$ base form
AVN–CTAB	9.62	5.32
AVN–TX-100	2.19	4.55
AVN–SDS	1.19	2.65

properties. Changes in the ionization constants were determined and compared with corresponding changes in enthalpies and entropies. These, in turn, have been attributed to a combination of electrostatic and hydrophobic interactions as well as H-bonding. Furthermore, association constant results support a model based on the above forces. Investigations are being carried out by the authors on structurally related azo dyes with the object of getting a better description of the dye–micelle interaction model.

Acknowledgements

The authors wish to thank the American University of Sharjah for the contribution and support to part of this work.

References

[1] Okwara M, Kitao T, Hirashima T, Mastsuoka M. Organic colorants. Tokyo: Kodanashu Ltd; 1988.
[2] Zollinger H. Color chemistry. New York: Weinheim, VCH; 1987.
[3] Waring DR, Hallas G. The chemistry and application of dyes. New York, London: Plenum Press; 1990.
[4] Zoolinger H. Azo and diazo chemistry: aliphatic and aromatic compounds. New York: Interscience Publishers; 1961.
[5] Dakiky M. PhD thesis. Charles University, Prague, Czech Republic; 1992.
[6] Fabian J, Hartmann HH. Light absorption of organic colorants. New York: Springer-Verlag; 1980.
[7] Gordon PF, Gregory P. Organic chemistry in colour. New York: Springer-Verlag; 1983.
[8] Hsieh BR, Denis D, Kazmair P. Dyes Pigments 1990;14:165.
[9] Dutta PK, Bhat SN. Colloids Surf A 1996;106:127.
[10] Pal P, Zeng H, Durocher G, Girard D, Giasson R, Blanchard L, et al. J Photochem Photobiol A Chem 1996;98:65.
[11] Buwalda RT, Jonker JM, Jan BF, Engberts N. Langmuir 1999;15(4):1083.
[12] Gonzalez AG, Herrador MA, Asuero AG. Anal Chim Acta 1991;246:429.
[13] Kendrick KL, Gilkerson WR. J Solution Chem 1987;16:257.
[14] Dakiky M, Nemacova I. Dyes Pigments 1999;40:141.
[15] Ramette RW. Chemical equilibrium and analysis. Reading, MA: Addison-Wesley; 1981 [Chapter 13].
[16] Bauer HH, Christian GD, O'Reilly JE. Instrumental analysis. New York: Allyn and Bacon; 1978.
[17] Fortune WB. In: Mellon MG, editor. Analytical absorption spectroscopy. New York: Wiley; 1950.
[18] Angelici RJ. Synthesis and technique in inorganic chemistry [Saunders Golden Sunburst Series]. 2nd ed. Philadelphia, Toronto: Saunders; 1977.
[19] Dakiky M, Nemacova I. Dyes Pigments 2000;44:181.
[20] Krpejsova L, Cermakova L, Podlahova J. Tenside Surfactants Deterg 1991;28:366.
[21] Dakiky M, Dweik H, Kanaan K, Kayali I, Khamis M, Manasra A, et al. J Al-Azhar Univ 1999;1(1):23.
[22] Dakiky M, Khamis M, Manasra A, Takrouri K. Color Technol 2002;118(4):191.
[23] Skarydova V, Cermakova L. Collection Czechoslovak Chem Commun 1982;47:1310.
[24] Simoncic B, Kovac F. Dyes Pigments 1999;40(1):1.
[25] Simoncic B, Span J. Dyes Pigments 1998;36(1):1.
[26] Esteve Romero JS, Ramis Ramos G, Garcia Alvarez-Coque MC. J Colloid Interface Sci 1991;11:141.
[27] Ramis Ramos G, Esteve Romero GS, Garcia Alvarez-Coque MC. Anal Chim Acta 1989;223:327.
[28] Bracko S, Span J. Dyes Pigments 2000;45:97.
[29] Mishra A, Patel S, Behera RK, Mishra BK, Behera GB. Bull Chem Soc Jpn 1997;70:2913.
[30] Jumean FH. J Indian Chem Soc 1986;63:967.
[31] Jumean FH, Khamis MI, Salaita GN. J Indian Chem Soc 1980;11:995.
[32] Dutta RK, Bhat SN. Bull Chem Soc Jpn 1993;66:2457.
[33] Pilipenko AT, Savransky LI. Talanta 1987;34(1):77.
[34] Jumean FH, Qaderi MI. J Indian Chem Soc 1988;65:41.
[35] Fasman GD, editor. Handbook of biochemistry and molecular biology, vol. 1. Cleveland: CRC Press; 1976. p. 153–262.
[36] Bates RG, Robinson RA. In: Conway BE, Barradas RG, editors. Chemical physics of ionic solutions. New York: Wiley; 1966. p. 211–35.
[37] Mukerjee P, Mysels KJ. Critical micelle concentrations of aqueous surfactant systems. Natl Stand Ref Data Ser Natl Bur Stand. Washington: US Government Publishing Office; 1971. [DC 20402 v + 222].
[38] Gehlen MH, Boens N, de Schryver FC, Van der Auweraer M, Reekmans S. J Phys Chem 1992;96:5592.